Title
PHOTOPRODUCTION OF NEUTRAL PIONS AS A FUNCTION OF MASS NUMBER

Authors
Andersen, John D.
Goodwin, Lester K.
Kenney, Robert W.

Publication Date
1960-11-04

UCRL-9465
Limited distribution

UNIVERSITY OF CALIFORNIA
Lawrence Radiation Laboratory
Berkeley, California
Contract No. W-7405-eng-48

PHOTOPRODUCTION OF NEUTRAL PIONS AS A FUNCTION OF MASS NUMBER

John D. Anderson, Lester K. Goodwin, and Robert W. Kenney
November 4, 1960

PHOTOPRODUCTION OF NEUTRAL PIONS AS A FUNCTION OF MASS NUMBER

John D. Anderson, Lester K. Goodwin, and Robert W. Kenney

Lawrence Radiation Laboratory
University of California
Berkeley, California

November 4, 1960

ABSTRACT

The relative yield of neutral photopions from various elements has been determined as a function of the quantum limit energy of the Berkeley synchrotron. Single decay photons from neutral pions were observed at 45, 90, and 135 deg to the incident bremsstrahlung in the laboratory system. Mean free paths for neutral pions in nuclear matter have been obtained, an optical model prediction of the photopion yields based upon pion-nucleus scattering data has been confirmed, and the presence of coherent pion production in the forward direction has been detected.

PHOTOPRODUCTION OF NEUTRAL PIONS[*] AS A FUNCTION OF MASS NUMBER

John D. Anderson, Lester K. Goodwin, and Robert W. Kenney

Lawrence Radiation Laboratory
University of California
Berkeley, California

November 4, 1960

I. INTRODUCTION

The existence of a neutral pion was first inferred by Bjorklund, Crandall, Moyer, and York from observations of high-energy gamma rays coming from targets bombarded by 340-Mev protons.[1]

Panofsky et al. were the first to study the photoproduction of neutral pions from complex nuclei in the region within 100 Mev of threshold; they observed energy and angular distributions and found that the meson yield was proportional to nuclear area.[2] Many investigators have studied both neutral- and charged-pion production from complex nuclei and have quite generally confirmed and also extended the early results of Panofsky et al.[3] Most recently, Davidson has measured neutral-photopion angular distributions for a number of elements, discussed coherent production, and placed a lower limit on the π^0 lifetime.[4] Leiss and Schrack have studied the problem of coherent π^0 production and its dependence upon nuclear size.[5]

The relation between yield and nuclear area has been discussed in terms of an optical model by Brueckner, Serber and Watson.[6] The nucleus is regarded as a sphere possessing a refractive index and an attenuation constant, the latter being expressed in terms of λ, the mean free path for absorption of pions in nuclear matter.

A mean free path of one to two times r_0 is inferred from the $A^{2/3}$ dependence of the 85-Mev π^0 production established by Panofsky, Steinberger, and Steller.

---

[*] This work was done under the auspices of the U.S. Atomic Energy Commission.

On the other hand, Hales and Moyer[7] were able to infer a mean free path of $10r_0$ for the absorption of 40-Mev neutral pions produced by proton bombardment of complex nuclei. These results indicate a strong dependence of the mean free path upon energy for the case of neutral pions in nuclear matter. However, in deriving mean free paths from the copius data on production of pions by protons on complex nuclei,[8] one must take into account the mean free path of protons in nuclear matter as well as Coulomb effects,[9] all of which make interpretation difficult.

The value of λ measured by Tenney and Tinlot[10] from scattering of charged pions on complex nuclei has a strong energy dependence varying from $12r_0$ to $3r_0$ for pion energies between 20 and 70 Mev, where the nuclear radius R is given by $R = r_0A^{2/3}$. This energy dependence, as analyzed by Stork,[11] was found to be the same as in the production of π^+ mesons in complex nuclei by incident protons.[12]

In π^+ photoproduction, Mozley[13] and Littauer and Walker[14] found a $Z/A^{1/3}$ dependence for the total pion yield at pion energies in excess of 65 Mev, which leads again to a small value of λ for charged pions at pion energies above 50 Mev.

Butler has pointed out alternatively that the $Z/A^{1/3}$ dependence of the charged photopion cross section for all values of λ could be explained on the basis of preferential surface production of pions.[15] This effect arises from a mechanism postulated by Wilson, in which a photopion produced within the nuclear volume is immediately reabsorbed by its parent nucleon and another nucleon with which the parent is interacting at the moment.[16] The results of Imhof[8] for charged pions are in sufficiently good agreement with optical-model predictions that it appears unnecessary to invoke the surface-production model.

In our work, the production of neutral photopions was studied as a function of mass number and of the photon energy at three laboratory angles in order to investigate the π^0 mean free path in the nucleus for photon energies near threshold, to observe the coherent production in the forward direction, and to test the validity of a result of Francis and Watson.[17] These latter authors have applied the optical model to the pion—complex—nucleus system and have shown that the Z dependence of photoproduction is the same as that for pion scattering from complex nuclei.

This work bears out the strong energy dependence of pion mean free paths inferred from the work of Panofsky[2] and of Hales and Moyer.[7] It indicates the presence of coherent production of neutral pions and reasonably well confirms the result of Francis and Watson.[17]

II. METHOD

Experimental information about interaction cross sections of neutral pions with nuclei must be inferred from production experiments because of the short π^0 mean life. From the various methods of observing π^0 production, the counting of single decay photons was chosen because the relatively high counting rates to which the method gives rise make it especially convenient for measuring ratios of yields.[18]

The 340-Mev bremsstrahlung beam from the Berkeley synchrotron was incident upon targets of various elements, and a counter telescope was used to detect single decay photons at laboratory angles of 45, 90, or 135 deg. The apparatus is shown in Fig. 1.

At intermediate pion energies ($T_\pi \cong 70$ Mev), the decay photons preserve the direction of the parent pion closely, so that at intermediate energies one measures relative values of $d\sigma/d\Omega$ when observing relative yields of single decay photons. Even at $T_\pi = 25$ Mev, the photon flux per unit solid angle at 45 deg to the π^0 direction in the laboratory system is one third its value at 0 deg.

An upper limit was placed upon the energy of the observed pions by selecting a different maximum photon energy of the synchrotron for successive runs. The relation between pion energies and the bremsstrahlung quantum-limit energy is discussed below.

III. APPARATUS AND PROCEDURE

The counter telescope (Fig. 1) consisted of three plastic scintillators and a lucite Čerenkov radiator viewed by RCA 6810 photomulitpliers. The first and third scintillators measured 6 by 7 by 1 in.. The second scintillator, which determined the telescope aperture, was 4 by 5 by 1 in. and subtended a solid angle of 0.05 sr at the target. The first scintillator was an anticoincidence counter which rejected all counts due to charged particles incident upon the telescope.

The counter was surrounded by 4 in. of lead, except for a 4- by 4- by 4- in. beryllium entrance window through which the counter telescope viewed the target. The beryllium attenuated the π^0 decay photons by approximately 15%, and its thickness exceeded the range of 100-Mev charged pions. The beryllium also reduced the number of low-energy electrons reaching the counters. A 1/2-inch-thick aluminum absorber was located between scintillators No. 2 and No. 3 to restrict further the response of the telescope to low-energy electrons.

Each scintillator was viewed through a 3.5-in. -long lucite light pipe in order to achieve a light-collection efficiency that was uniform to within 20% over the entire volume of the scintillator.

To show that photons from π^0 decay were being detected, the counting rate of the photon telescope was measured as a function of bremsstrahlung quantum-limit energy and of the thickness of the lead converter. The lead transition curve (see Fig. 2) fits the expected curve very well and yields a mass-absorption coefficient of 0.09 cm^2/g, which is in agreement with the absorption coefficient of 100-Mev photons in lead. The zero point on the transition curve is estimated on the basis of the pair conversion due to the first scintillator.

The meson target was removed, and the counting rate fell by a factor of 80. When the bremsstrahlung quantum-limit energy was decreased, the counting rate decreased in accordance with the excitation function for neutral pions, and when the quantum-limit energy was lowered below threshold, the yields were zero within statistical error.

The yield of decay photons was observed at three laboratory angles as a function of the atomic weight for a series of targets and also as a function of the quantum-limit energy, k_{max}, of the synchrotron (five such energies were used). The energy k_{max} was determined by measuring the high-energy end of the bremsstrahlung spectrum with a high-resolution three-channel pair spectrometer. This instrument augmented the thin-wall precollimator monitor chamber and the Cornell thick-wall monitor chamber in assuring stability of synchrotron operation.

The distribution of beam in time was monitored by a scintillator placed along the beam center line. The duration of the beam was approximately 1 msec, centered at the peak magnetic field of the synchrotron. The energy spread of the electrons striking the target was less than 1% due to the spread in time of the electrons striking the synchrotron internal target.

Data were taken with the lead converter in place in the scintillation telescope as well as with it removed; the counting rate due to photons is given by the difference of these two observed rates. The net counting rate was negligibly small when the quantum-limit energy of the synchrotron bremsstrahlung was below the π^0 threshold. The accidental counting rate was held below 1% on all runs by limiting the synchrotron beam intensity.

A block diagram of the electronics is shown in Fig. 3. A minimum-ionizing particle passing through a scintillator gave a 2-v negative pulse into a 125-ohm cable. The pulses were amplified and limited in Hewlett-Packard 460 wide-band amplifiers, and were then fed into a distributed triple-coincidence circuit equipped with a single anticoincidence input for the anticoincidence scintillator signal.

A (2, 3, Čerenkov) count signified that a photon converted into charged particles in the lead converter and the charged particles passed through the counter telescope. If a charged particle from the target passed through the entire telescope, the signal from the first (or anti) scintillator electronically cancelled the coincidence-circuit output.

Counting rate plateaus were plotted versus phototube voltage. They extended over several hundred volts for cosmic rays and were rechecked during the experiment by use of electrons from π^0 decay gammas converting in the beryllium window.

Accidental counts were held to a small fraction of the real counts through the use of closely fitting machined lead bricks to shield the counter, and by the reduction of the charged-particle flux with the 4-in.-thick beryllium window. All amplifiers and coincidence circuits were temperature-controlled and obtained their power from regulated 110-v sources to insure stability.

IV. TARGET CORRECTIONS

An upper limit of 5×10^{-16} sec to the mean life for decay of the neutral pion assures that the neutral-pion decays were very near to the nuclei in which they were produced.[19] The principal corrections to the data account for the absorption of both incident bremsstrahlung and pion decay photons in the targets and vary between 10 and 20%, depending upon the element in question. The uncertainties in these photon-absorption corrections are 2% for light elements, increasing to 3% for the heaviest elements. The corrected data and their accompanying errors are shown in Figs. 4, 5, and 6.

V. RESULTS AND DISCUSSION

The validity of an application of the optical model to the photoproduction of neutral pions in complex nuclei can be tested by using the results of Francis and Watson, in which they show that the differential cross section for the production of photopions exhibits the same dependence upon atomic number in complex nuclei as the pion total-absorption cross section in complex nuclei.[17] In order to effect this comparison, the various known experimental pion total absorption cross sections[20] at each of several incident pion energies, were plotted as a function of lnA. Weighted least-squares fits of straight lines were made to the data at each pion energy, T_π. Some examples are shown in Fig. 7. The fitted slope for each pion energy was then plotted in Fig. 8 as a function of the "equivalent energy" of the bremsstrahlung, $K_{eq} = T_\pi + \mu c^2$, where K_{eq} is taken equal to the quantum limit energy of the bremsstrahlung beam, k_{max}. The smooth curve drawn between the points in

Fig. 8 then describes the dependence of the pion scattering upon A. It is to be compared with values of the slopes, n, of lines fitted to relative cross sections for corrected neutral-pion production at various laboratory production angles and for several different quantum-limit energies, k_{max}, of the incident bremsstrahlung. Table I lists the least-squares values of n and λ/r_0 at laboratory angles of 45, 90, and 135 deg for various values of T_π. Figures 4, 5, and 6 show the least-squares fitted curves and their associated errors. The slope, n, of the photopion-yield curves depends very weakly upon k_{max}, so that $k_{max} = T_\pi + \mu c^2$ was taken to be the proper value for the comparison with scattered pions of kinetic energy T_π. The excitation function for π^0 production from a given element is not simply related to the relative yields at a given angle. The efficiency of the photon counter changes by approximately 50% over the photon energy range, and the uncertainty in the π^0 angular distributions reflect sufficient uncertainty in the π^0 decay spectra at any given observation angle that no attempt was made to extract an excitation function from the data.

In order to compare these various data over the complete energy range under discussion, the slopes of the straight lines fitted to the π^0 yield curves in Figs. 5, 6, and 7 are shown plotted versus k_{max} for laboratory angles of 45, 90, and 135 deg in Figs. 9, 10, and 11. Superimposed upon these points is the curve giving the corresponding slope for pion-scattering data in Fig. 8. It is seen that the agreement is reasonable for angles of 135 and 90 deg.

The 45-deg yield data show marked disagreement with the pion-scattering data. It is concluded that the validity of the optical model as applied to neutral photopion production at large angles is borne out by the 90- and 135-deg data. The π^0 yields at 45 deg in the laboratory system are considerably greater than would be expected from the optical-model comparison with pion scattering. The optical-model considerations are not sufficient then to account for this forward π^0-production data. The enhanced yield at 45 deg is due to coherent production, that process which involves the nucleus recoiling as a whole in its ground state. The coherent π^0- production amplitude is given by the sum of partial amplitudes from all nucleons in the nucleus. Its contribution to the total production cross section varies with A^2, and the angular distribution is sharply peaked near the forward direction. The data do not include sufficiently complete angular distributions to observe quantitative details of the coherent production.

In the attempt to estimate the absorption mean free path of neutral pions in nuclear matter, the optical-model calculations of Brueckner, Serber, and Watson[6] were applied to the 90- and 135-deg π^0 yields. The yield per nucleon is the product of the probability of a nucleon's producing a pion and the probability of the pion's escaping the nucleus. Brueckner et al. have averaged over the nuclear volume the probability that a pion will escape the nucleus if its production probability is assumed constant throughout the nucleus.[6] The probability of escape is given by

$$f(A, \lambda) = 3 \left[1/2\,x - 1/x^3 + 1/x^3\,(1 - x)e^{-x} \right],$$

where $x = 2R/\lambda$. Here we have the nuclear radius $R = r_0 A^{1/3}$, and λ is the pion mean free path in nuclear matter. For 50-Mev neutral pions the mean free path for pion-nucleon scattering within nuclear matter (including charge exchange) is estimated to be 12 r_0, and the scattering mean free path increases with decreasing pion energy. Since the mean free path for scattering is large compared with λ, the λ is just the mean free path for absorption, and the yield per nucleon is then proportional to the escape probability $f(A, \lambda)$.

Values for the π^0 mean free path were derived from the data for each energy and laboratory angle by making a weighted least-squares fit of the function $f(A, \lambda)$ to the data. Figures 4, 5, and 6 compare the fitted functions with the data points. The derived values of λ for all cases are given in Table I with their errors from the least-squares analysis.

The values of λ derived from this experiment at 90 and 135 deg are in reasonable agreement with those obtained by Imhof[8] from the photoproduction of positive pions from complex nuclei. These values are also in reasonable agreement with the values obtained by Stork[11] and by Tenney and Tinlot[10] from analysis of charged-pion scattering on complex nuclei. Figure 12 compares the results of this experiment with π^0 optical-model predictions corrected for pion scattering within the nuclear medium as proposed by Frank, Gammel, and Watson,[21] and corrected by Watson and Zemach[22] for more-accurate nuclear-radius measurements. The potentials of Frank, Gammel, and Watson have been used to relate the pion energy within the nucleus to its laboratory energy after passing through the nuclear surface.[21] These potentials are for charged pions; π^0 mean free paths are expected to be twice that for the corresponding charged-pion case if it is assumed that pion capture occurs on virtual deuterons in the nucleus. The processes inverse to capture are $p + p \rightarrow \pi^+ + d$, and $n + p \rightarrow \pi^0 + d$; the charged cross section[23] is the greater by a factor of 2. Accordingly, the calculated charged-pion mean free paths have been doubled for presentation in Fig. 12. The optical-model predictions[17] and these experimental results are in quite general agreement, including our derived mean free paths, which have quite large statistical errors.

ACKNOWLEDGMENTS

The authors wish to express their gratitude to Professors Edwin M. McMillan and A. Carl Helmholz for their advice and encouragement throughout the course of this work. We are indebted to Dr. C. A. McDonald for many interesting and helpful discussions during the planning and execution of this experiment. Thanks are due Mr. Duane Gates and Mr. William Swanson for assistance in taking data. We also thank Mr. Rudin Johnson and the synchrotron crew for their efficient handling of the machine.

REFERENCES

1. Bjorklund, Crandall, Moyer, and York, Phys. Rev. 77, 213 (1950).
2. Panofsky, Steinberger, and Steller, Phys. Rev. 86, 185 (1952).
3. Lindenfeld, Sachs, and Steinberger, Phys. Rev. 89, 531 (1953); G. Cocconi and A. Silverman, Phys. Rev. 88, 1230 (1952); Calvin G. Andre, The Photoproduction of π^0 Mesons from Hydrogen and Deuterium (thesis), Lawrence Radiation Laboratory Report UCRL-2425, November 1953; Bingham, Keck, and Tollestrup, Bull. Am. Phys. Soc. 30, No. 1, T3 (1954); Goldwasser, Koester, and Mills, Phys. Rev. 95, 1692L (1954); Imhof, Knapp, Easterday, and Perez-Mendez, Phys. Rev. 108, 1940 (1957).
4. Gilbert Davidson, Photoproduction of Neutral Mesons from Complex Nuclei (thesis), Massachusetts Institute of Technology Report MIT-LNS-TR-72, September 1959.
5. J.E. Leiss and R.A. Schrack, Revs. Modern Phys. 30, 456 (1958).
6. Brueckner, Serber, and Watson, Phys. Rev. 84, 258 (1951).
7. R.W. Hales and B.J. Moyer, Phys. Rev. 89, 1047 (1953).
8. D. Clark, Phys. Rev. 81, 313 (1951); J. Merritt and D. Hamlin, Phys. Rev. 96, 638 (1955).
9. S. Gasiorowicz, Phys. Rev. 93, 843 (1954).
10. F.H. Tenney and J. Tinlot, Phys. Rev. 92, 974 (1953).
11. D.H. Stork, Phys. Rev. 93, 868 (1954).
12. S. Leonard and D.H. Stork, Phys. Rev. 93, 568 (1954).
13. R.F. Mozley, Phys. Rev. 80, 493 (1950).
14. R.M. Littauer and D. Walker, Phys. Rev. 82, 746 (1951).
15. S.T. Butler, Phys. Rev. 87, 1117 (1952).
16. R.R. Wilson, Phys. Rev. 86, 125 (1952).
17. N.C. Francis and K.M. Watson, Phys. Rev. 89, 328 (1953).

18. G. Cocconi and A. Silverman, Phys. Rev. 88, 1230 (1952).

19. M. Jacob and J. Mathews, Phys. Rev. 117, 854 (1960).

20. R. L. Martin, Phys. Rev. 87, 1052 (1952); D. H. Stork, Phys. Rev. 93, 868 (1954); Chedester, Isaacs, Sachs, and Steinberger, Phys. Rev. 82, 958 (1951).

21. Frank, Gammel, and Watson, Phys. Rev. 101, 891 (1956).

22. K. Watson, and C. Zemach, Kinematics of Meson Interactions within Nuclei, Lawrence Radiation Laboratory Report UCRL-8355, June 1958.

23. A. H. Rosenfeld, Phys. Rev. 96, 139 (1954).

Table I. Least-squares fitted values of n and λ/r_0 at laboratory angles of 45, 90, and 135 deg for various pion energies

Pion energy (Mev)	Quantum limit energy (Mev)	45 deg		90 deg		135 deg		Run No.
		n	λ/r_0	n	λ/r_0	n	λ/r_0	
30	165					0.872±.057	12.4±102.2	1
30	165	1.77±.10	∞	1.04±.04	23.6±62.1	1.30±.14	∞	2
42	177					0.824±.030	5.43±2.86	1
55	190	1.40±.11	∞	0.96±.07	5.80±4.14	0.93±.11	5.53±6.80	2
65	200	1.37±.22	∞					2
70	205					0.795±.020	1.29±.25	1
95	230			0.84±.08	4.99±3.94			2
120	255					0.756±.015	1.45±.23	1
205	340					0.745±.012	1.63±.25	1
205	340	0.80±.03	2.32±.26	0.64±.04	0	0.77±.01	2.10±.27	2

FIGURE LEGENDS

Fig. 1. Schematic diagram of the experimental setup.

Fig. 2. Transition curve for the lead converter in the counter telescope.

Fig. 3. Block diagram of the electronics.

Fig. 4. Relative π^0 yield <u>vs</u> mass number at 45 deg (lab).

Fig. 5. Relative π^0 yield <u>vs</u> mass number at 90 deg (lab).

Fig. 6. Relative π^0 yield <u>vs</u> mass number at 135 deg (lab).

Fig. 7. Pion total-absorption cross sections for various nuclei and pion energies. The straight lines are least-squares fitted to the data. Their slopes and errors are shown.

Fig. 8. Slope of the pion absorption with respect to mass number <u>vs</u> the equivalent peak energy of the bremsstrahlung.

Fig. 9. Slope of the π^0 yield with respect to mass number at 45 deg (lab) <u>vs</u> the peak energy of the bremsstrahlung. The dotted line corresponds to the solid line of Fig. 8.

Fig. 10. Slope of the π^0 yield with respect to mass number at 90 deg (lab) <u>vs</u> the peak energy of the bremsstrahlung. The dotted line corresponds to the solid curve of Fig. 8.

Fig. 11. Slope of the π^0 yield with respect to atomic weight at 135 deg (lab) <u>vs</u> the peak energy of the bremsstrahlung. The dotted line corresponds to the solid curve of Fig. 8.

Fig. 12. Mean free path of a neutral pion in nuclear matter <u>vs</u> pion energy. The curves are those of Frank, Gammel, and Watson, and of Watson and Zemach corrected for neutral pions.

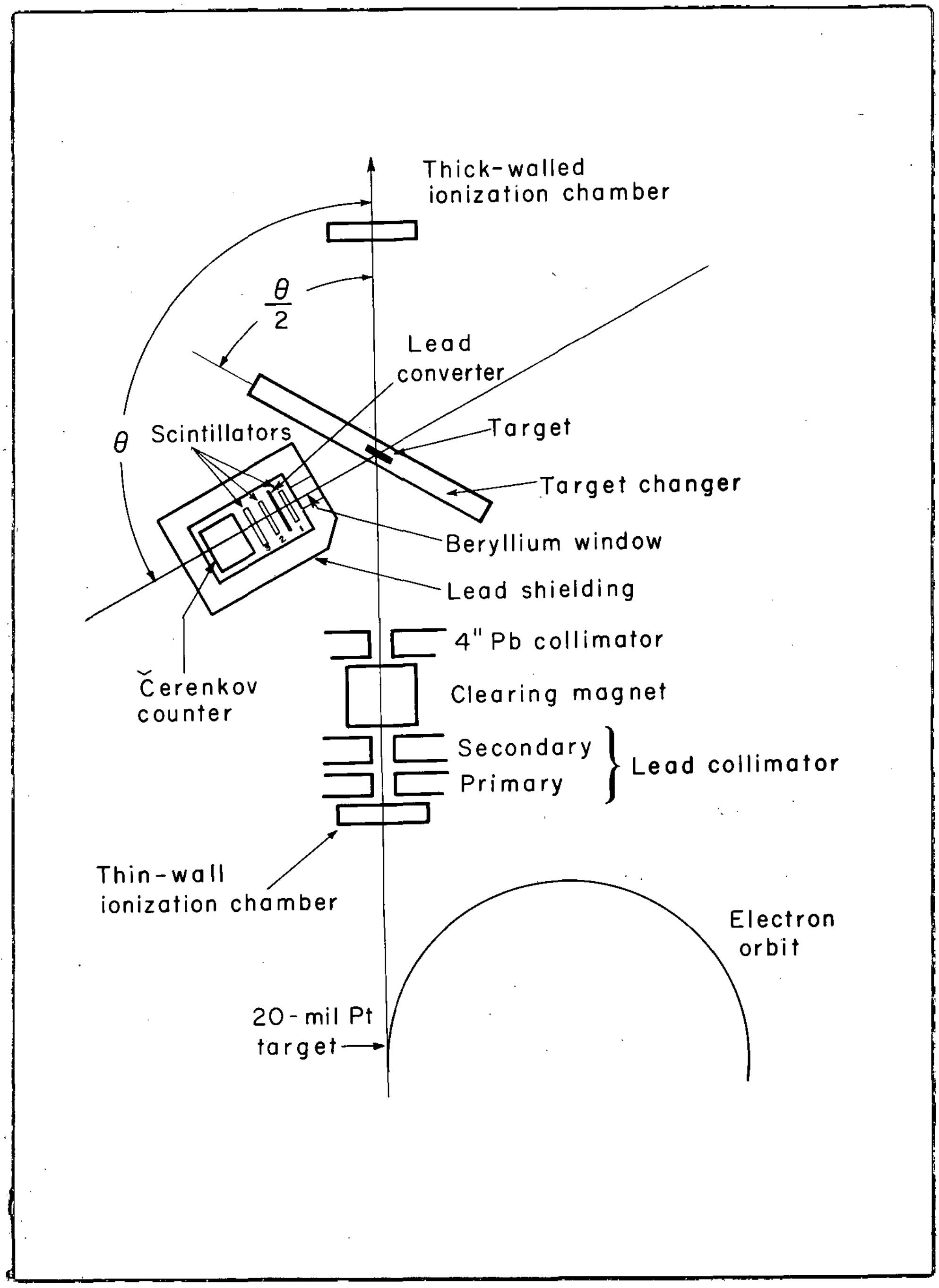
Thick-walled ionization chamber
θ/2
θ
Lead converter
Scintillators
Target
Target changer
Beryllium window
Lead shielding
4" Pb collimator
Čerenkov counter
Clearing magnet
Secondary
Primary
Lead collimator
Thin-wall ionization chamber
Electron orbit
20-mil Pt target

Fig. 1

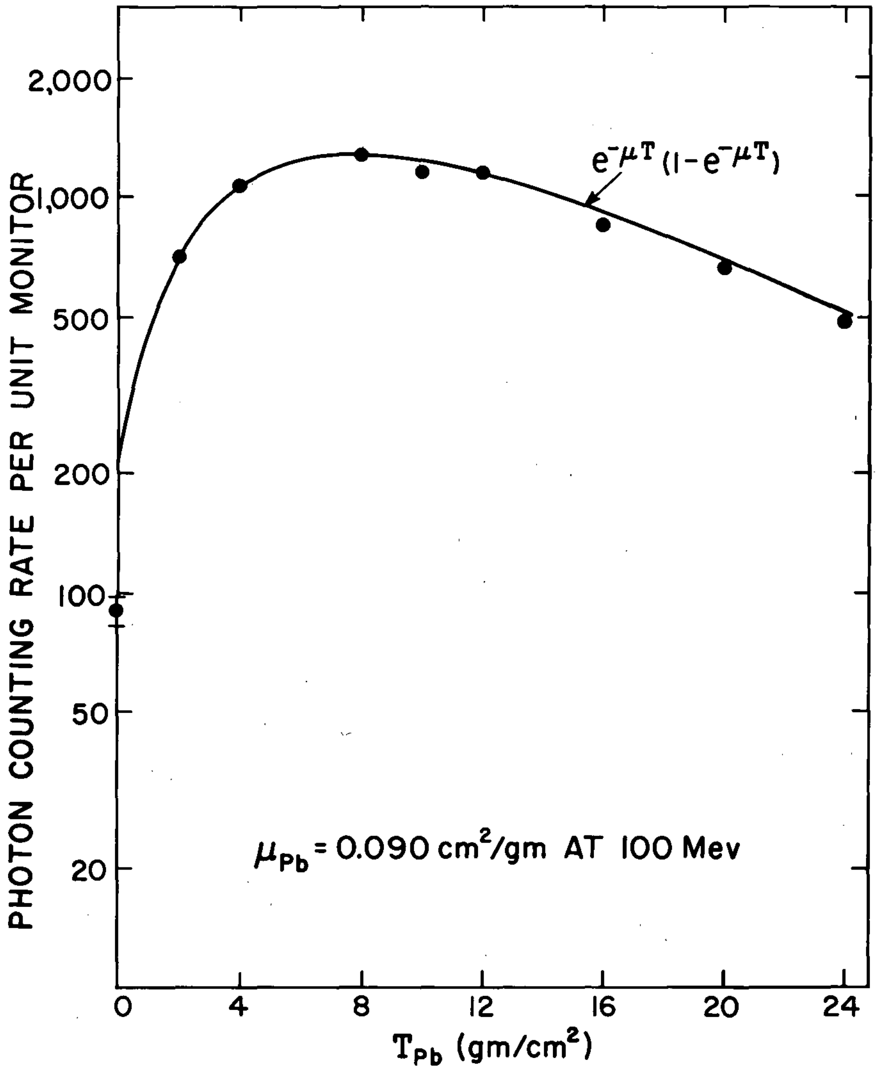
PHOTON COUNTING RATE PER UNIT MONITOR
2,000
1,000
500
200
100
50
20
$e^{-\mu T}(1-e^{-\mu T})$
$\mu_{Pb} = 0.090\ cm^2/gm$ AT 100 Mev
0
4
8
12
16
20
24
$T_{Pb}\ (gm/cm^2)$

Fig. 2

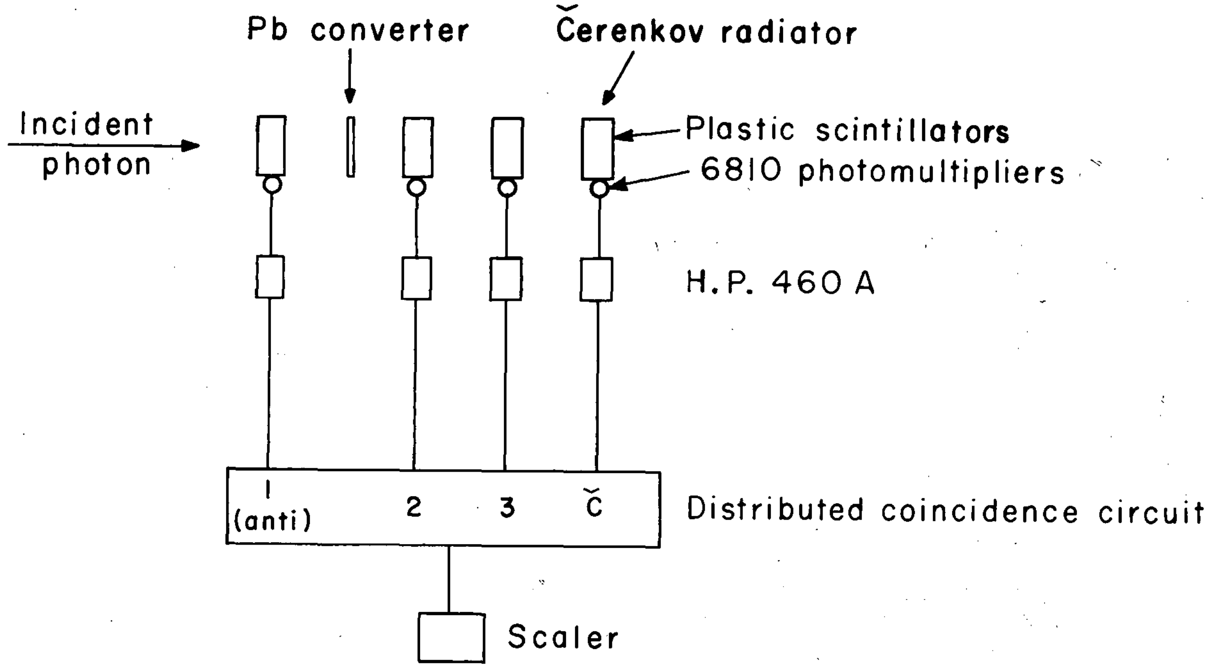
Pb converter
Čerenkov radiator
Incident photon
Plastic scintillators
6810 photomultipliers
H.P. 460 A
1 (anti)
2
3
Č
Distributed coincidence circuit
Scaler

Fig. 3

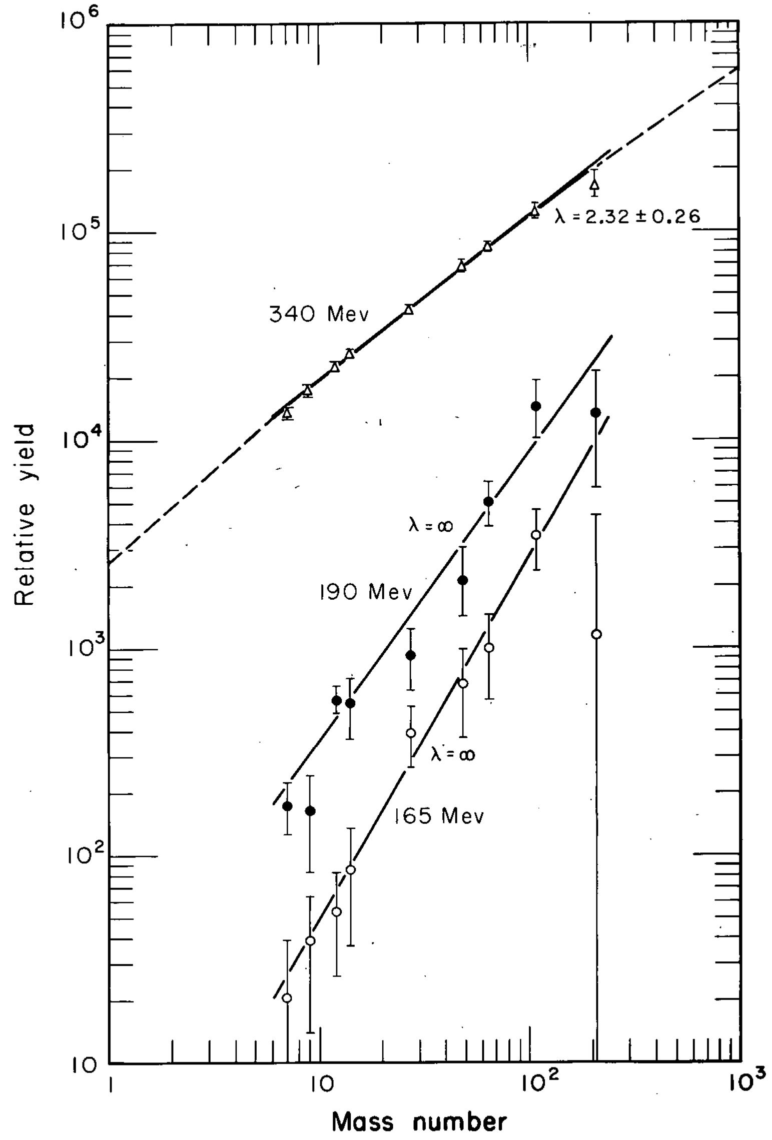

Relative yield
Mass number
10
10²
10³
10⁴
10⁵
10⁶
1
10
10²
10³
340 Mev
λ = 2.32 ± 0.26
190 Mev
λ = ∞
165 Mev
λ = ∞

Fig. 4

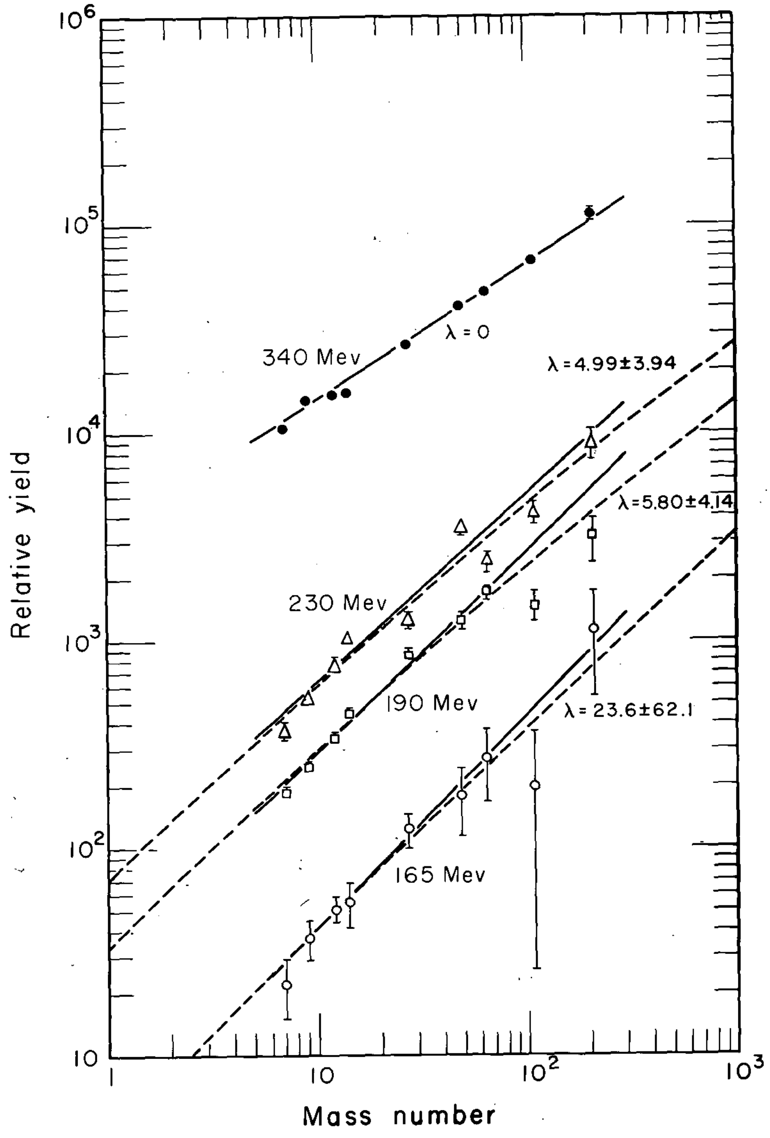

10^6
10^5
10^4
10^3
10^2
10
1
10
10^2
10^3
Relative yield
Mass number
340 Mev
λ = 0
λ=4.99±3.94
230 Mev
λ=5.80±4.14
190 Mev
λ= 23.6±62.1
165 Mev

Fig. 5

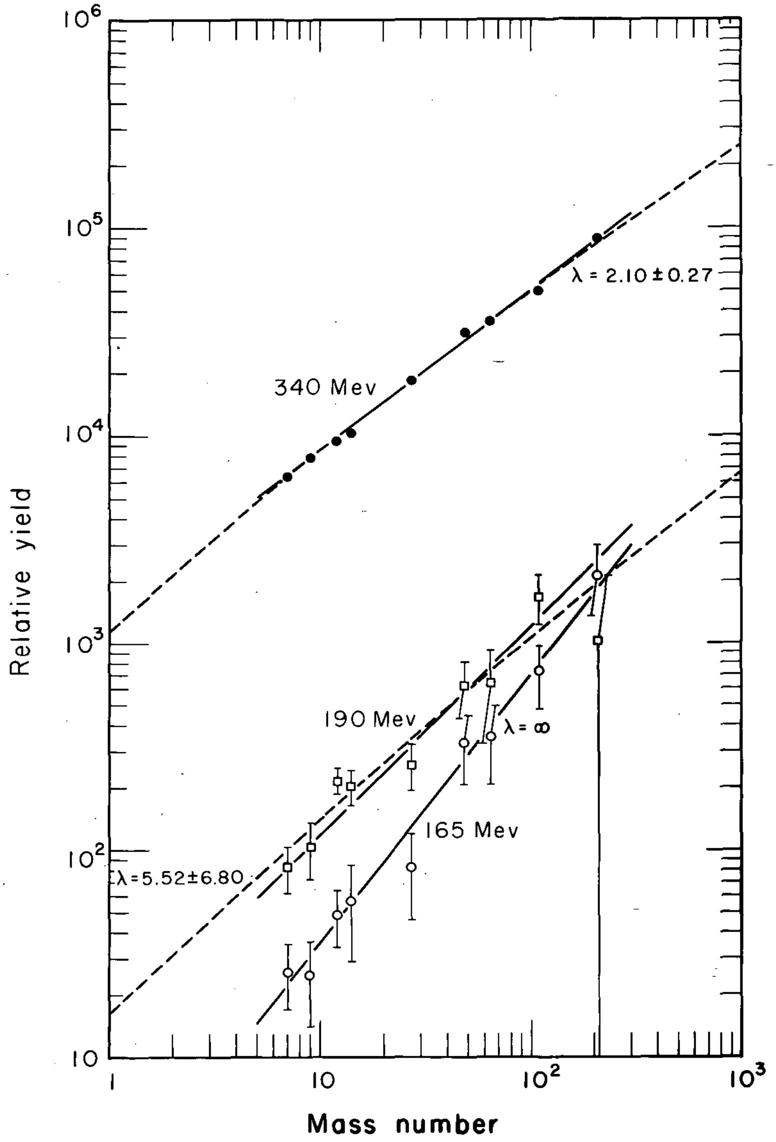
10⁶
10⁵
10⁴
10³
10²
10
1
10
10²
10³
Relative yield
Mass number
340 Mev
λ = 2.10 ± 0.27
190 Mev
λ = ∞
165 Mev
λ=5.52±6.80

Fig. 6

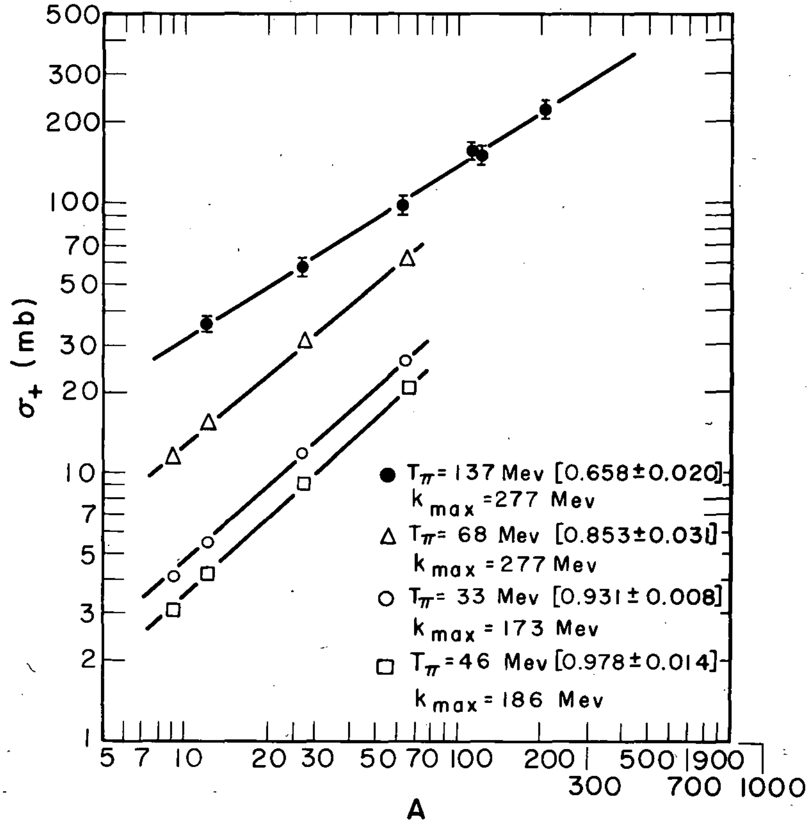
σ_+ (mb)
500
300
200
100
70
50
30
20
10
7
5
3
2
1
5 7 10 20 30 50 70 100 200 300 500 700 900 1000
A
● T_π = 137 Mev [0.658±0.020]
k_{max} = 277 Mev
△ T_π = 68 Mev [0.853±0.031]
k_{max} = 277 Mev
○ T_π = 33 Mev [0.931±0.008]
k_{max} = 173 Mev
□ T_π = 46 Mev [0.978±0.014]
k_{max} = 186 Mev

Fig. 7

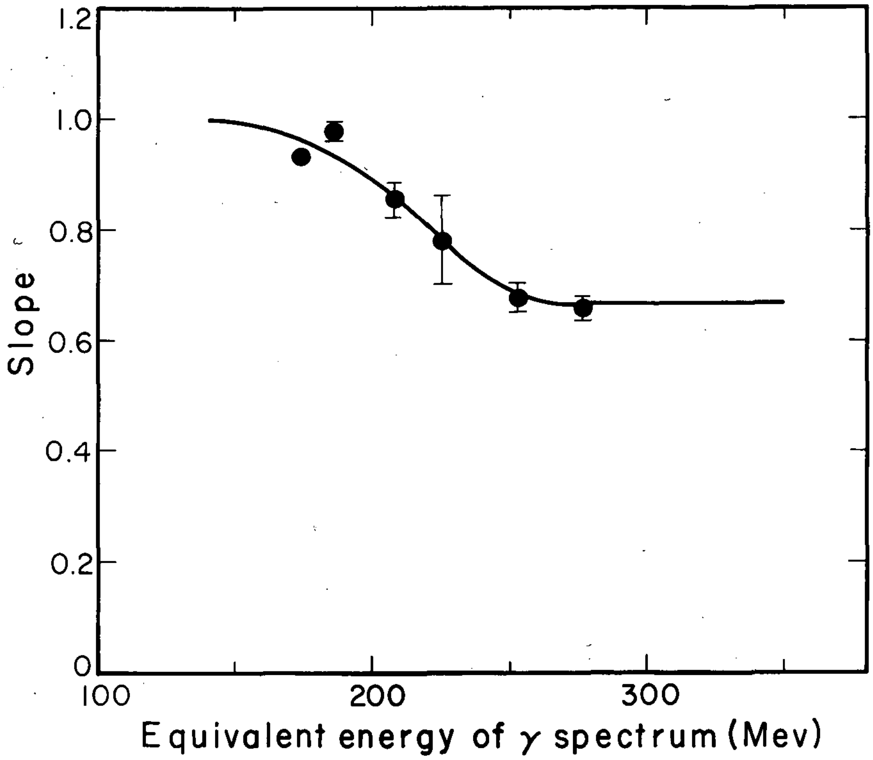
1.2
1.0
0.8
0.6
0.4
0.2
0
Slope
100
200
300
Equivalent energy of γ spectrum (Mev)

Fig. 8

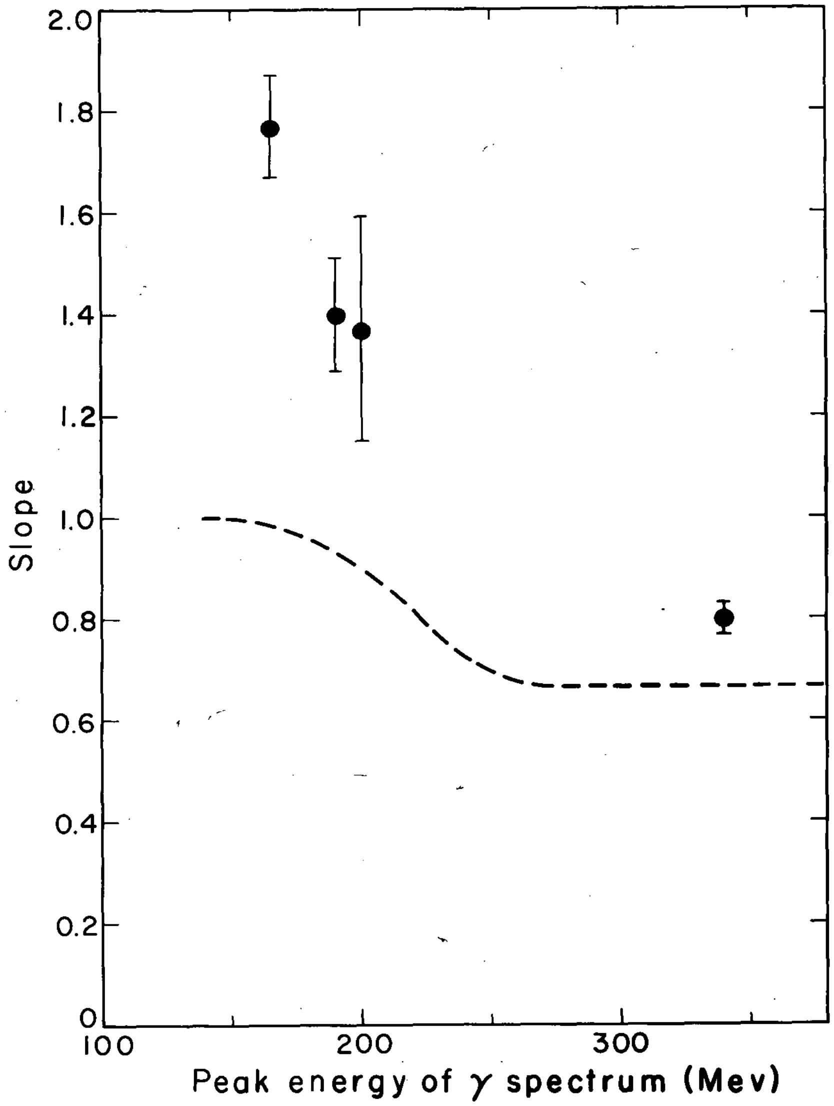
2.0
1.8
1.6
1.4
1.2
1.0
0.8
0.6
0.4
0.2
0
Slope
100
200
300
Peak energy of γ spectrum (Mev)

Fig. 9

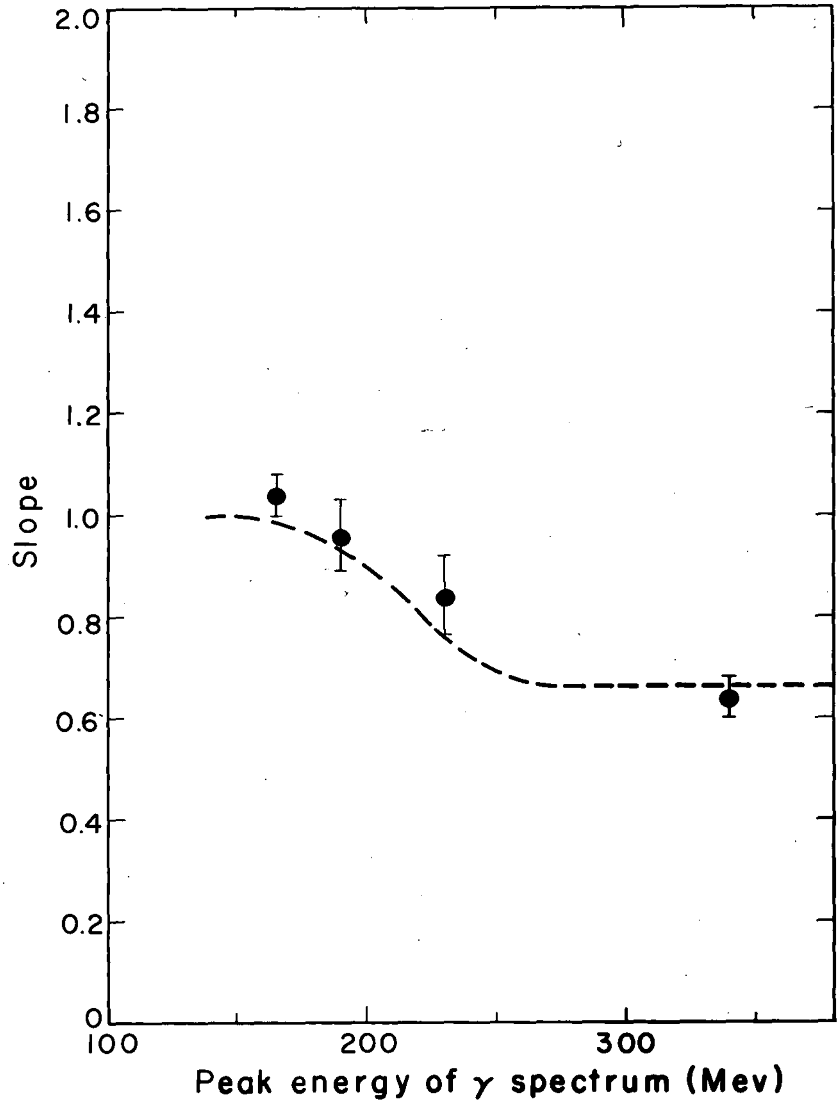
2.0
1.8
1.6
1.4
1.2
1.0
0.8
0.6
0.4
0.2
0
Slope
100
200
300
Peak energy of γ spectrum (Mev)

Fig. 10

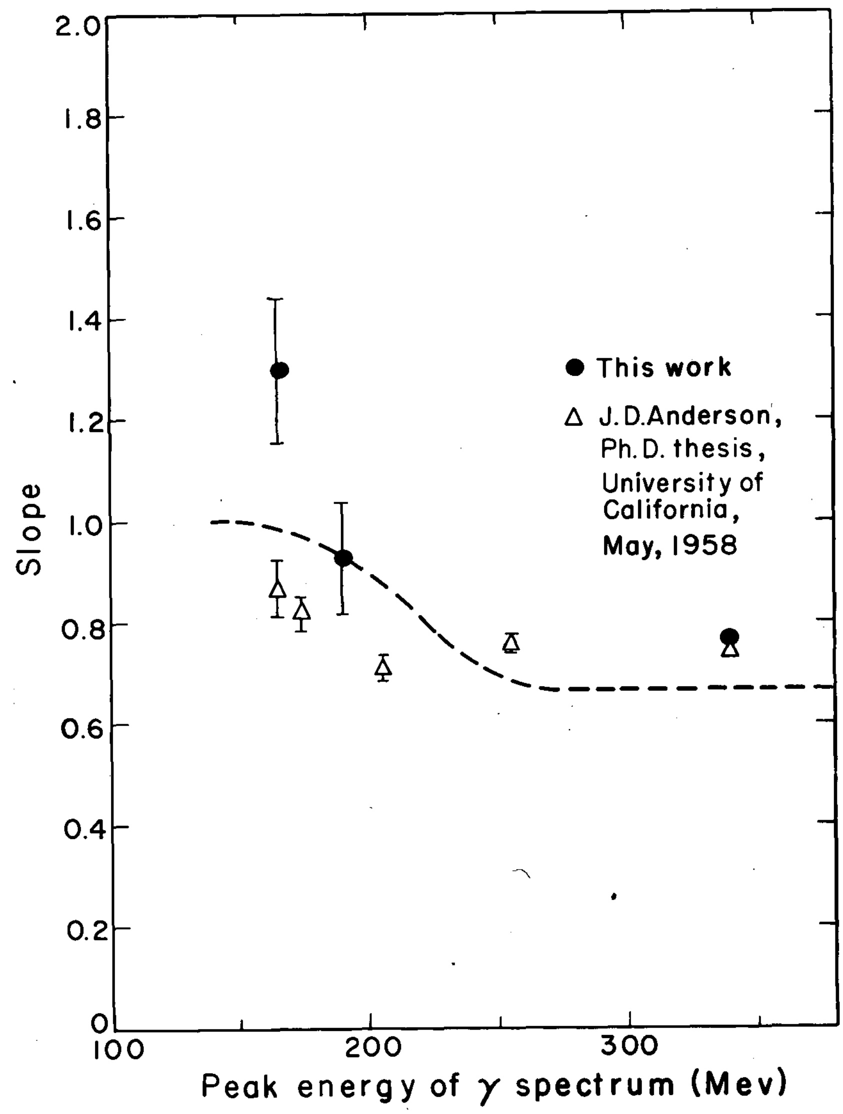
2.0
1.8
1.6
1.4
1.2
1.0
0.8
0.6
0.4
0.2
0
Slope
100
200
300
Peak energy of γ spectrum (Mev)
● This work
△ J.D.Anderson, Ph.D. thesis, University of California, May, 1958

Fig. 11

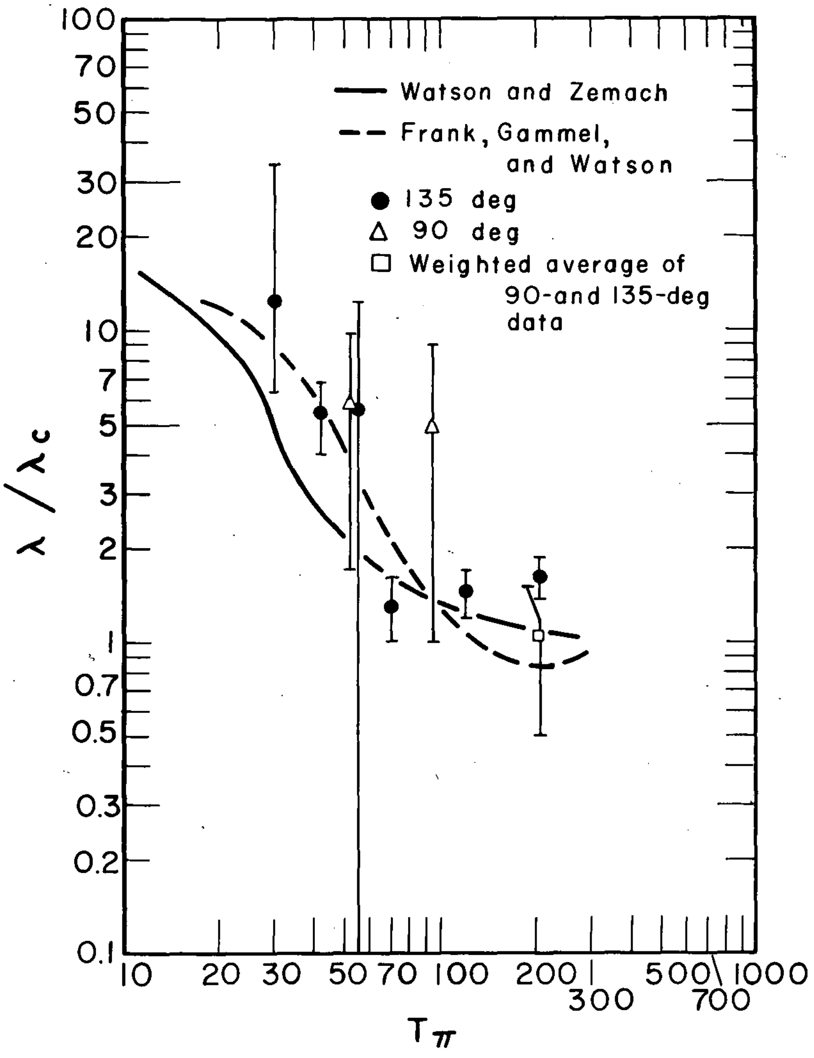
100
70
50
30
20
10
7
5
3
2
1
0.7
0.5
0.3
0.2
0.1
λ/λ_c
10
20
30
50
70
100
200
300
500
700
1000
T_π
Watson and Zemach
Frank, Gammel, and Watson
● 135 deg
△ 90 deg
□ Weighted average of 90-and 135-deg data

Fig. 12